CIRCULATION IN GAS-SLURRY COLUMN REACTORS: SECOND QUARTERLY REPORT, QUARTER ENDING MARCH 31, 1988

WEST VIRGINIA UNIV., MORGANTOWN. DEPT.
OF MECHANICAL AND AEROSPACE ENGINEERING

1988

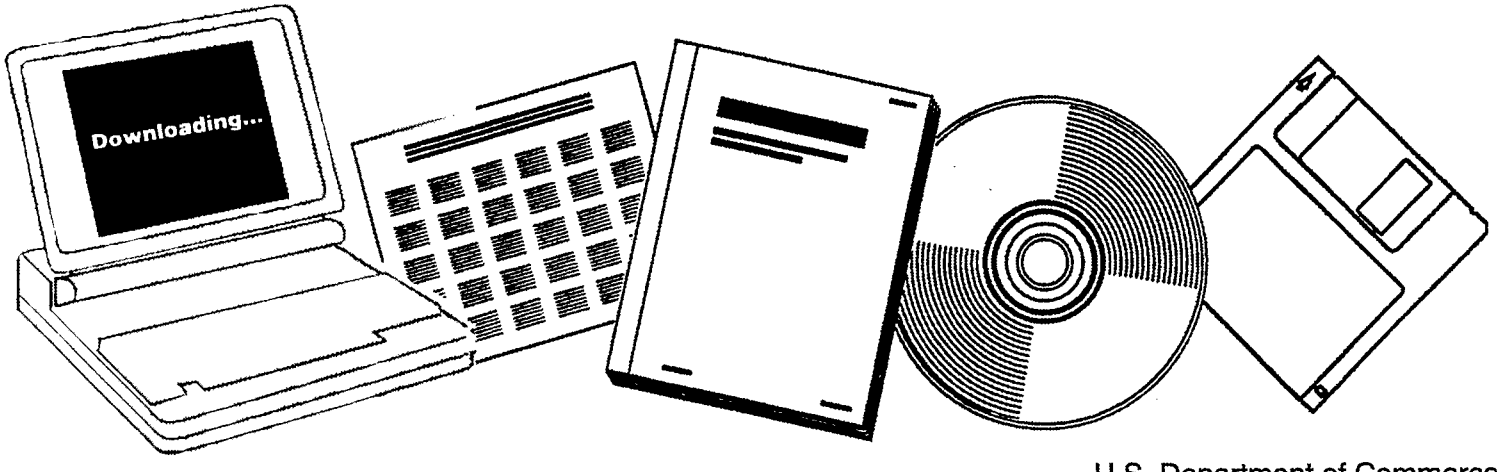

One Source. One Search. One Solution.

NTIS

Providing Permanent, Easy Access to U.S. Government Information

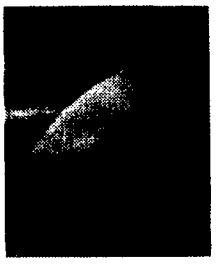

National Technical Information Service is the nation's largest repository and disseminator of government-initiated scientific, technical, engineering, and related business information. The NTIS collection includes almost 3,000,000 information products in a variety of formats: electronic download, online access, CD-ROM, magnetic tape, diskette, multimedia, microfiche and paper.

Search the NTIS Database from 1990 forward

NTIS has upgraded its bibliographic database system and has made all entries since 1990 searchable on **www.ntis.gov.** You now have access to information on more than 600,000 government research information products from this web site.

Link to Full Text Documents at Government Web Sites

Because many Government agencies have their most recent reports available on their own web site, we have added links directly to these reports. When available, you will see a link on the right side of the bibliographic screen.

Download Publications (1997 - Present)

NTIS can now provides the full text of reports as downloadable PDF files. This means that when an agency stops maintaining a report on the web, NTIS will offer a downloadable version. There is a nominal fee for each download for most publications.

For more information visit our website:

www.ntis.gov

U.S. DEPARTMENT OF COMMERCE
Technology Administration
National Technical Information Service
Springfield, VA 22161

LEGIBILITY NOTICE

A major purpose of the Technical Information Center is to provide the broadest dissemination possible of information contained in DOE's Research and Development Reports to business, industry, the academic community, and federal, state and local governments.

Although a small portion of this report is not reproducible, it is being made available to expedite the availability of information on the research discussed herein.

DE88013080

DOE/PC/79935--4

DOE/PC/79935—4

DE88 013080

"CIRCULATION IN GAS-SLURRY COLUMN REACTORS"

DEPARTMENT OF ENERGY. CONTRACT NUMBER DE-FG22-87PC79935

SECOND QUARTERLY REPORT - REPORT DOE/PC/7935-4
QUARTER ENDING 3/31/88

Prepared by

WEST VIRGINIA UNIVERSITY

DEPARTMENT OF MECHANICAL AND AEROSPACE ENGINEERING

Principal Investigators:
Nigel Clark
John Kuhlman
Ismail Celik

Prepared for

DEPARTMENT OF ENERGY, PITTSBURGH

TABLE OF CONTENTS

SUMMARY

In this quarter the 20cm diameter laboratory bubble column has been constructed and tested with air–water operation. Theory has been developed based on experimental measurement of bubble shapes to predict bubble size distribution from probe measurements. In addition, an experimental technique for acquiring a global force balance on a bubble column has been used and data from this work are currently being processed.

Numerical simulation of two phase systems has commenced. During the next quarter resistance and vacuum probe data will be acquired from the new column, the laser doppler velocimeter will be assembled and tested at the column, and numerical modeling of a laminar circulating system will proceed.

INTRODUCTION

During this second quarter of research into bubble column circulation, the major research effort has been devoted to the construction of the large experimental column, which is now complete. The computational modeling effort is now underway and some detailed theory on probe signal interpretation has been developed using experimentally acquired bubble shape parameters. In addition, a balance technique has been employed in an attempt to measure average wall shear in the column, but current results are preliminary and show that these forces may be difficult to measure.

Vacuum probe research and Laser Doppler Velocimetry are about to commence now that the column is constructed.

Details of the research achievements follow in the next chapter.

TECHNICAL ACHIEVEMENTS

COLUMN CONSTRUCTION

The large column has been constructed in accordance with the design presented in the last quarterly report, DOE/PC/79935-2. A drawing of the column is repeated here in Figure 1. To date this column has been tested with water and minor leaks have been repaired. The first two phase tests are commencing at the present time.

PROBE RESEARCH

No experimental research has been undertaken directly with resistance probes during this quarter. However, there has been significant advance in the theory to interpret probe signals as bubble size distributions, as is related below. Part of this research has been submitted for the 3rd International Symposium on Liquid-Solid Flows, and involved both theoretical and experimental work.

BUBBLE VELOCITY

A resistance probe signal yields the time interval for which a bubble envelops the probe, so that we must know a relative velocity between the bubble and probe in order to calculate the chord length which the probe cuts through the bubble. In a very fast flow, an homogenous model (gas velocity equal to slurry or liquid velocity) and an assumed velocity profile may yield a satisfactory result. At low or moderate velocities or in circulating bubble columns, the local bubble velocity can be calculated only with a knowledge of slurry or liquid velocity and bubble slip. Otherwise, "twin probes," such as those of Herringe & Davis (1978) must be used to yield not only the time interval, but also the bubble velocity, the latter quantity being found from a cross-correlation of the two signals from the two probes.

A further case involves the rise of relatively few bubbles through a

quiescent medium, where it is known that bubbles over a wide range of volumes have very similar velocities. Bubble rise velocity in this region (diameters 2 to 30mm) is given by the equation of Harmathy (1960).

$$U = 1.53 \left[\frac{g(\rho_L - \rho_G)\ \sigma}{\rho_L^{\ 2}} \right]^{0.25}$$

(1) or the equation of Levich (1962)

$$U = 1.41 \left[\frac{g\ (\rho_L - \rho_G)\ \sigma}{\rho_L^{\ 2}} \right]^{0.25}$$

CHORD LENGTHS

Let us assume that a knowledge of local bubble velocity has permitted the calculation of many chord lengths, each representing a bubble intersecting the probe for some time interval. These chord lengths are usually different from the bubble size (no matter how it is defined) because bubbles will not generally be pierced by the probe at their centers. Yamashita et al (1979), Werther (1974) and Clark & Turton (1988) have presented analyses to deal with this problem and to convert a chord length distribution into a bubble size distribution. In order to do this, one needs to assume a bubble shape to permit geometric analysis. For example, Werther assumes that spherical cap bubbles in fluidized beds could functionally be approximated by ellipsoids while Clark & Turton (1988) discussed truncated ellipsoids as a general bubble shape to represent spherical, ellipsoidal, cap and spherical cap bubbles. However, these analysis assumed that all of the bubbles had the same fundamental shape, regardless of size. In this new research, the change of shape with size typical of gas bubbles rising in a liquid or slurry was considered.

Figure 2 shows a probe cutting an ellipsoidal bubble, together with notation used in this report below.

BUBBLE SHAPES AND EXPERIMENTAL WORK

Surface tension dominates the forces on very small bubbles, so that they are quite spherical. Bubbles (in water) larger than 2 to 3mm experience distortion by the pressure field surrounding them and are flattened to assume an ellipsoidal shape. It is this shape which increases the drag on the bubble so that an increase in rise velocity with increase in bubble volume is lower than might be expected. Ellipsoidal shapes persist over an order of magnitude in diameter, while separation of the boundary layer from even larger bubbles yields the familiar cap-shaped bubble with a smooth zenith and a disordered wake.

Although it is acknowledged that bubble shape is dependent on surface tension, we used in this research typical size-shape relationships found in air-water systems. Jones (1965) has published photographs of air bubbles in water which are also reproduced in Batchelor's book (1977). These pictures have been carefully measured to yield the chord length, y, at up to 20 points across the bubble diameter. Height was always measured vertically, diameter horizontally. Let us assume that these bubbles may be functionally modeled as ellipsoids with a major (horizontal) axis of 2R, and a minor (vertical) axis of $2\alpha R$. To find the most representative value of the aspect ratio α for each bubble, a regression routine was applied to the measurements of each bubble to yield both α and the best locus of the center of the bubble diameter. Figure 3 shows this translation for one particular bubble. Once α was available for each bubble variation of α over a limited range of bubble size, R, was found through regression using an equation of the form

$$1/\alpha^2 = a_1 R + b_1 \qquad (1)$$

In the case of Jones' bubbles, an even simpler fit valid for the ellipsoidal shape region was evident

$$1/\alpha^2 = a_2 R \qquad (2)$$

Results for Jones' Bubbles are shown in Figure 4, together with a best fit line of $1/\alpha^2 = 0.512$ R (in mm). Other forms for the regression equation are clearly possible and are being investigated.

Detailed data on bubble shape are also available in a paper by Harmathy (1960). He has plotted the bubble aspect ratio $1/\alpha$ against the Eotvos number,

$$Eo = \frac{g\,(\rho_L - \rho_G)d^2}{\sigma}$$

and the reader is referred to his paper to find bubble shapes in unusual fluid combinations. For air-water systems, Harmathy's "best-fit" line is in poor agreement (see figure 5) with our measurements of Jones' bubbles, although it must be noted that there was considerable scatter of data about the best fit curve in Harmathy's paper. It is also not clear that Harmathy used the same protocols to measure bubbles and find their aspect ratio as we did, and it is well documented that the condition of the water affects the shape by modifying the surface tension.

In addition we acquired some of our own bubble shape data by photographing single bubbles in a 6 inch diameter glass column containing tapwater. A Nikon camera with a narrow depth of field (focus) at the column center was employed and distortion of shape by the round column was corrected by also photographing a metal scribed plate lowered into the column of water. Once again, bubble shapes were measured to yield a best fit value of α, as shown in figure 6. This data showed good agreement with the best fit line through harmathy's data, given by

$$a_2 = 1.15 mm^{-1}$$

so that this value for a_2 was chosen for use below.

In considering Fischer-Tropsch reactors, modeling bubble shape in inviscid liquids is inappropriate, so that other gas-liquid or gas-slurry systems must be explored to gain a general bubble shape relationship. Bubble shapes were also photographed in viscous sugar solutions, where bubble aspect ratio was more pronounced. Raw data are given in figures 7-9 and will be considered in detail during the next quarter.

Using this model of ellipsoidal approximation of bubble shape, one can proceed with an analysis of probe signals to find bubble size distribution.

ANALYSIS

Consider a swarm of bubbles rising past a probe, which may intersect some of the bubbles at distances r from their centers. The probability that intersection of a bubble of radius R occurs at radius r is

$$P(r/R) = 2r/R^2 \text{ for } 0 \leq r \leq R \qquad (3)$$

and is zero otherwise. If we know the bubble shape for a specific size R (for example an ellipsoid of known α) we can predict the chord length, y, which is cut by the probe at radius r. The resultant probability density function is given by Clark and Turton (1988) as

$$P(y/R) = P(r/R) \left|\frac{dr}{dy}\right| = (2r/R^2)\left|\frac{dr}{dy}\right| \qquad (4)$$

When there is a range of bubble sizes present, we may measure the same chord length y by cutting a small bubble close to its center or a large bubble near its edge. Whereas the probability of measuring a chord length y on a bubble of particular size R in the population of bubbles touching the probe is given by

$$P(y,R) = P(y/R)P(R) \qquad (5)$$

the probability of measuring y for any size of bubble is

$$P(y) = \int^{\infty} P(R)\, P(y/R)dR \qquad (6)$$

which, for constant α, would yield [18]

$$P(y) = \frac{1}{2\alpha^2 R_{max}^2} \left[(2\alpha R_{max} - y) \right] \qquad (12)$$

For the variable values of α as expressed in equations 1 and 2

$$P(y) = \int_{\frac{a_1 y + \sqrt{a_1^2 y^4 + 16 b y^2}}{8}}^{R_{max}} \frac{y(a_1 R + b_1)}{2R^2} \cdot \frac{1}{R_{max}} \, dR \qquad (13)$$

$$= \frac{y}{2R_{max}} \left\{ a_1 \log \left(\frac{8R_{max}}{a_1 y^2 + \sqrt{a_1^2 y^4 + 16 b_1 y^2}} \right) - \frac{b_1}{R_{max}} + \frac{8b_1}{a_1 y^2 + \sqrt{a_1^2 y^4 + 16 b_1 y^2}} \right\}$$

and

$$P(y) = \int_{\frac{a_1 y^2}{4}}^{R_{max}} \frac{y a_2}{2R^2} \frac{1}{R_{max}} \, dR \qquad (14)$$

$$= \frac{y a_2}{2 R_{max}} \log \left[\frac{4R_{max}}{a_2 y^2} \right]$$

Both equations 13 and 14 have a lower limit of validity for y. Below this limit equations 1 and 2 are inappropriate descriptors of bubble shape, since they do not predict the spherical shape of small bubbles.

One can also consider the case of a uniform bubble size distribution in the system, $P_S(R) = \frac{1}{R_{max}}$, in which case the distribution of bubble sizes touching the probe is given by:

$$P(R) = \frac{3R^2}{R_{max}^3} \tag{15}$$

and using equation (1)

$$P(y) = \frac{3y}{4R_{max}^3}\left[a_1R_{max}^2 + 2b_1R_{max} - \frac{a_1}{64}\left[a_1y^2 + \sqrt{a_1y^4 + 16b_1y^2}\right]^2 \right.$$

$$\left. \frac{-b_1}{4}\left[a_1y^2 + \sqrt{a_1y^4 + 16b_1y^2}\right]\right] \tag{16}$$

or using equation (2)

$$\text{or } P(y) = \left[a_1R_{max}^2 - \frac{a_1}{16}(a_1^2y^4)\right] \tag{17}$$

Thus far we have demonstrated the calculation of a chord length distribution for a given bubble size distribution. However, the researcher is more interested in the reverse procedure, which must be tackled numerically. Following the technique proposed previously by Clark and Turton (1988), we will consider grouping our measured chord lengths into m partitions each embracing a range of chord lengths Δy.

Let us divide the chord lengths into equal length partitions such that

$$y_i = y_{max} - (i+1/2)\,\Delta y \quad 0 < m-1 \text{ where } \Delta y = \frac{y_{max}}{m}$$

Then an approximation to the probability of finding a chord length y between y_i and y_{i+1} $W(y_i < y < y_{i+1})$, is given by

$$W(y_i < y < y_{i+1}) = \int_{y_i}^{y_{i+1}} P(y)\,dy = \int_{y_i}^{y_{i+1}} \int_0^{R_{max}} P(y/R)P(R)dRdy \tag{18}$$

$$\propto \sum_{j=0}^{m-1} \int_{y_i}^{y_{i+1}} P(y/R_j)dy \;\; P(R_j) \triangle R$$

Hence

$$W_i = W(y_i < y < y_{i-1}) \propto \sum_{j=0}^{m-1} C_{i,j} \; P(R_j) \triangle R$$

where (19)

$$C_{i,j} = \int_{y_i}^{y_{i+1}} P(y/R_j) \; dy$$

and

$$R_j = R_{max} - j\triangle R \qquad o \leq j \leq m-1$$

with $\triangle R = \frac{R_{max}}{m} = \frac{y_{max}}{2\alpha m}$

Equation (19) can be used to construct the following triangular matrix form:

$$W_o = C_{o,o} \; P(R_o)\triangle R$$

$$W_1 = C_{1,o} \; P(R_o) \; \triangle R + C_{1,1} \; P(R_1) \; \triangle R$$

$$\vdots$$

$$W_{m-1} = C_{m-1,o} \; P(R_o) \; \triangle R + C_{m-1,1} \; P(R_1)\triangle R + \ldots + C_{m-1,m-1} \; P(R_{m-1}) \; \triangle R$$

The triangularity occurs because $C_{i,j}$ is zero when i is smaller than j, i.e. a chord length y_i can only arise from a bubble of radius R_i or greater (R_{i-1}, R_{i-2}, etc.). For a known bubble shape $C_{i,j}$ is known and the W_i are calculated from the chord length data. One constraint is that we must assume that the largest chord length measured is representative of the largest bubble encountered by the probe. Thus the above matrix can be solved sequentially to yield the unknown $P(R_i)$.

EXAMPLE OF A BACK-TRANSFORM

Five thousand chord length observations were generated synthetically using Monte Carlo simulation. A triangular bubble size distribution was assumed with mode = 18mm and range $0 \leq R \leq 30$mm. Bubble shape was calculated using equation 2 with $a_2 = 1.15\text{mm}^{-1}$. The generated distribution of chord lengths is shown in figure 10. The backward transformation was carried out on the data and the resulting probability density function for R is compared with the actual bubble size distribution in figure 11. This comparison of the actual distribution and the backward transformation is good and illustrates the utility of this technique. (Note that one should compare the upper right corners of each histogram with the original distribution).

Clark and Turton (1988) have commented on possible instability of this type of matrix transform. If too few bubbles are measured and too many size distribution intervals chosen, an oscillatory solution may result and even negative probabilities may be found. This undesirable effect is accentuated in this case when the bubbles change shape with size. Also, in the limit where bubble height remains constant although horizontal diameter changes, it becomes impossible to infer the horizontal diameter from measurements of the vertical height. Fortunately, in reality, bubble shape does not change that dramatically as a function of size, although the deformation does not favor the back-calculation of diameter. Figures 12 and 13 illustrate an attempt to infer a bubble size distribution using 10 discrete sizes from 5000 chord length observations. Instability is evident in the solution.

During this quarter a technique has been devised whereby bubble size distribution can be calculated from a measured distribution of vertical chord lengths cut by a probe through a sufficiently large number of bubbles of varying size and shape. This represents an advance over previous work,

where bubble shape was assumed to be invariant with respect to size.

The technique as presented above suffers the limitation that the change of bubble shape with size cannot be explained by one linear equation. At very small radii, the shape is constant, while at large radii, transition from the ellipsoid to the cap-shape occurs. Values for P(y/R) for spheres and cap (Taylor) bubbles have been given by Clark and Turton (1988) and could be incorporated into the matrix transform to broaden the valid bubble size range that could be inferred. However, even in a quiescent liquid or slurry, bubble rise velocity varies significantly over this broader range, so that the chord lengths themselves are more difficult to measure. Nevertheless, this relatively simple technique will permit more accurate processing of probe information in future circulation research.

GLOBAL FORCE BALANCE

In a separate endeavor, two senior students are currently attempting to measure wall shear and pressure at the base of the column to achieve a global experimental force balance on the column. As shown in the schematic in figure 14, average wall shear, Tw, is being measured with a clear plastic cylinder suspended from a balance arm inside an operating 6 inch diameter bubble column. Pressure is being measured at the base of the column with a static probe connected to an inclined manometer. At present the preliminary data suggests that the measured variables change weakly so that great accuracy cannot be expected. Full details of this effort will be available in the next report.

PROGRESS ON NUMERICAL MODELING

The VEST computer code (Leschziner, 1980; Stamou and Adams, 1985) has been loaded on the West Virginia computer network (WVNET) at West Virginia University. This computer code has been reviewed, tested, and modified for

axisymmetric, vertical, single-phase pipe flow. The vertical pipe used for the modification has a diameter of 0.4 meter and length of 25.0 meter. A laminar developing pipe flow with a Reynolds number Re = 100, and a uniform entrance velocity of 0.45×10^{-5} m/s had been successfully simulated using this modified version. The solution has conversed to a steady state solution in about 600 iteration with a mass residuce of 8×10^{-5} which is very good. The numerical results have been compared with analytical results. As shown in Fig. 15. The velocity distribution from the computer code for the fully developed flow at a distance of 62 diameters from the pipe inlet is identical with the theortical result. At this distance the flow is fully developed as expected. The predicted pressure drop and the wall friction also agree closely with the analytical results. However, numerically computed pressure gradient show some unexpected oscillaticns at the outflow boundary of the calculation domain. This problem is currently being investigated.

In the next quarterly period the governing equations for a two-phase non-reacting (isothermal) newtonian fluid flow will be reviewed. These equations will be compared witht he partial differential equations being solved in JVEST and a numerical solution scheme will be developed which utilizes the same techniques as in the present code. Preliminary review of the equations for multi-phase flows have been completed. The informaiton presented by Chan and Masiello (1986) for a water - water vapor two-phase system have been found very useful. The set of equations that will be solved for a water-air two-phase system will be presented in the next quarterly. Before starting the solution of these set of equations the boundary conditions for a water-air circulation tank in the bubbly flow regime will be studied in detail. In order to avoid further complications inherent to slug flows, and chun-turbulent flows, the initial stage of the numerical study will be limited to

homogeneous (bubbly) flow regime. This will be done by choosing parameters according to the empirically established transition criteria in the literature. Two examples of these are depicted in Fig. 16a and 16b.

PLANNED RESEARCH

In the next quarter the large laboratory bubble comumn will be operated with water over a range of superficial air velocities. Gas holdup wil be acquired with resistance probes and with the vacuum probe discussed in the last quarterly report. Liquid height will be varied in the column to determine whether multiple circulation cell operation will occur. The laser doppler velocimeter will be assembled in the multiphase flow laboratory adjacent to the column and it is hoped that the first LDV measurements of liquid velocity will be made.

Numerical modeling of laminar circulating systems will continue and available results will be compared with data in the literature.

Global force balance calculations wil be completed and reported in the next quarterly report.

Nomenclature

a_1, a_2, b_2	constants used in equations (1) and (2)
$C_{i,j}$	coefficient in matrix relating chord length to bubble size
d	diameter of equivalent volume sphere (m)
E_o	Eotvos number, $\frac{g(\rho_L - \rho_G)d^2}{\sigma}$
m	number of subdivisions
n	number of data points
P(r/R)	conditional probability density function for r under constraint of a given value of R (1/m)
P(R)	probability density function for bubble size distribution touching the probe (1/m)
P(y)	probability density function for measured chord lengths (1/m)
P(y,R)	Probability density function for encountering a bubble of size R and measuring a chord length y ($1/m^2$)
P(y/R)	conditional probability density function for chord length y under constraint of a given value of R (1/m)
$P_s(R)$	bubble size distribution in system (1/m)
r	radius at which probe pierces bubble (m)
R	radius of a bubble (m)
R_{max}	radius of largest bubble (m)
y	pierced chord length (m)
y_{max}	largest possible pierced chord length (m)
W_i	probability of finding a chord length y between y_i and y_{i+1}

greek letters

α	aspect ratios of ellipsoidal bubble
ρ	density (kg/m^3)
σ	surface tension (N/m)
$\Delta R, \Delta y$	represents the difference between successive bubble, chord sizes

subscripts

G	gas
i	denotes chord length in matrix
j	denotes bubble radius in matrix
L	liquid
max	maximum

REFERENCES

1. Harmathy, T.Z., "Velocity of Large Drops and Bubbles in Media of Infinite or Restricted Extent" A.I.Ch.E. Journal, Vol. 6, pp. 281-288, (1960).

2. Levich, V.G. Physical-Chemical Hydrodynamics, Prentice-Hall, New York, 1962.

3. Yamashita, F., Mori, Y. and Fujita, S., "Sizes and Size Distributions of Bubbles in a Bubble Column" Jour. Chemical Engineering of Japan, Vol. 12, pp. 5-9, (1979).

4. Werther, J. "Bubbles in Gas-Fluidized Beds" Trans. I. Chem. Engrs., Vol. 52, 149-169, (1974).

5. Clark, N.N. and Turton, R. "Chord Length Distributions Related to Bubble Size Distributions in Multiphase Flows" Int. Jour. Multiphase Flow, in press, (1988).

6. Jones, D.R.M., Ph.D. Dissertation University of Cambridge, 1965.

7. Batchelor, G.K. "An Introduction to Fluid Dynamics" Cambridge Univ. Press, London., (1977).

8. Stamou, A.I., and Adams, E., "Description of the VEST computer Code with Examples of Applications to Settling Tank." Report No.: SFB 210/T/16, Sonderforschungsbereich 210 University of Karlsruhe, F.R.G., November, (1985).

9. Chan, R. K-C., and Masiello, P.J., "PORTHOS—A Computer Code for Solving General Three-Dimensional, Time-Dependent Two-Fluid Equations," Presented at the Winter Annual Meeting, Anaheim, CA, Dec. 7-12, (1986).

10. Shah, Y.T., Kelkar, B.G., Godbole, S.P., and Deckwer, W.D., "Design Parameter Estimations for Bubble Column Reactors," AIChE J., 28(3), 353, (1982).

11. Dukler, A.E., Taitel, Y., "Flow Pattern Transitions in Gas-Liquid Systems: Measurement and Modeling," in Multiphase Science and Technology, editors: G.F. Hewitt, J.M. Dehhaye, and N. Zuber, Hemisphere Publishing Corp. New York, (1986)

12. Leschziner, M.A. "A Numerical Scheme for Simulating the Vertical Structure of Time-Dependent Natural Water Flows," Report No.: SFB 80/T/167, Sonderforschungsbereich 210 University of Karlsruke, F.R.G, (1980).

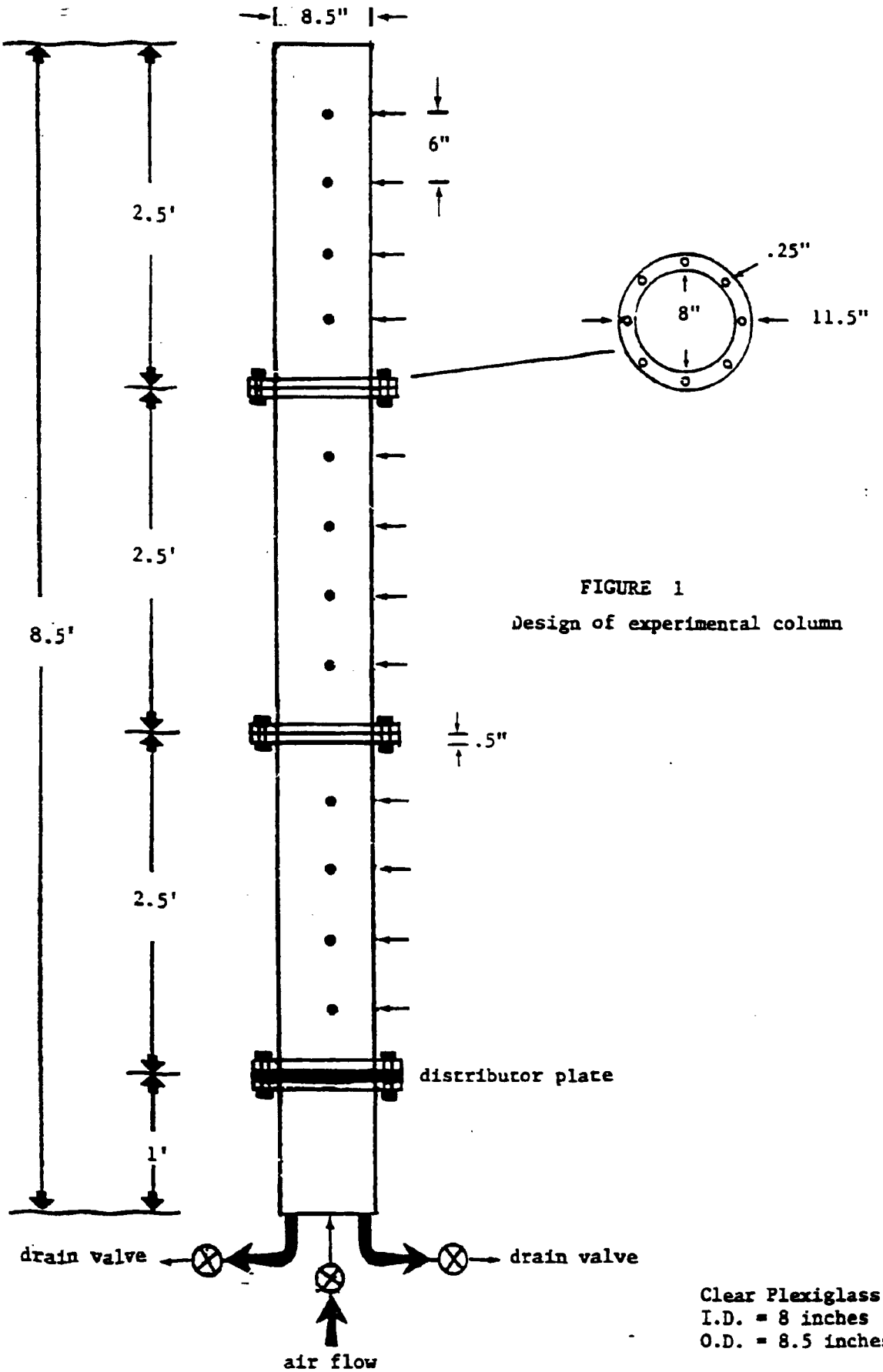

FIGURE 1

Design of experimental column

Clear Plexiglass Column
I.D. = 8 inches
O.D. = 8.5 inches

1 block approx. = 1.5"

● ← Probe Holes, 90° off

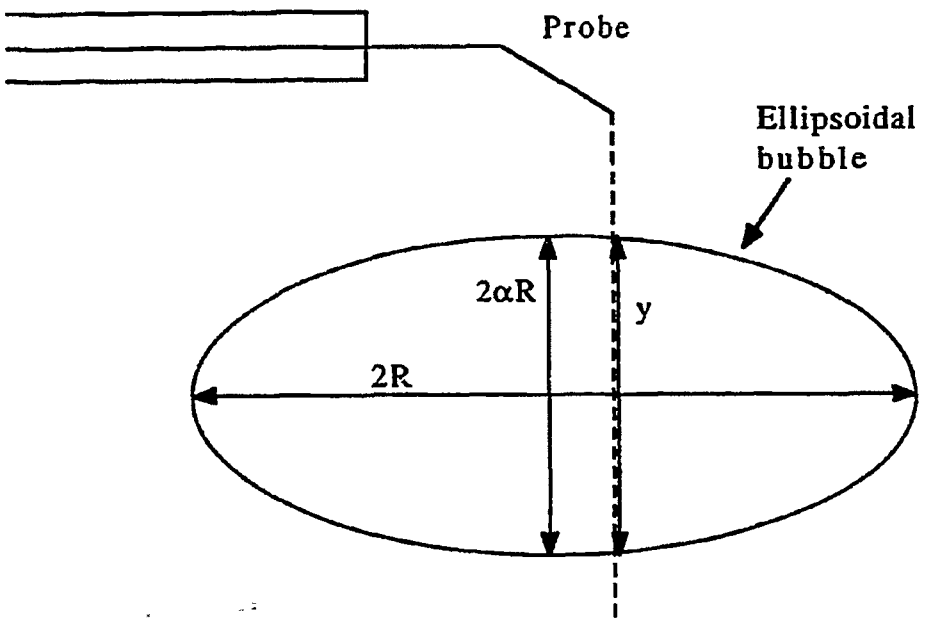

Figure 2

Probe cutting ellipsoidal bubble

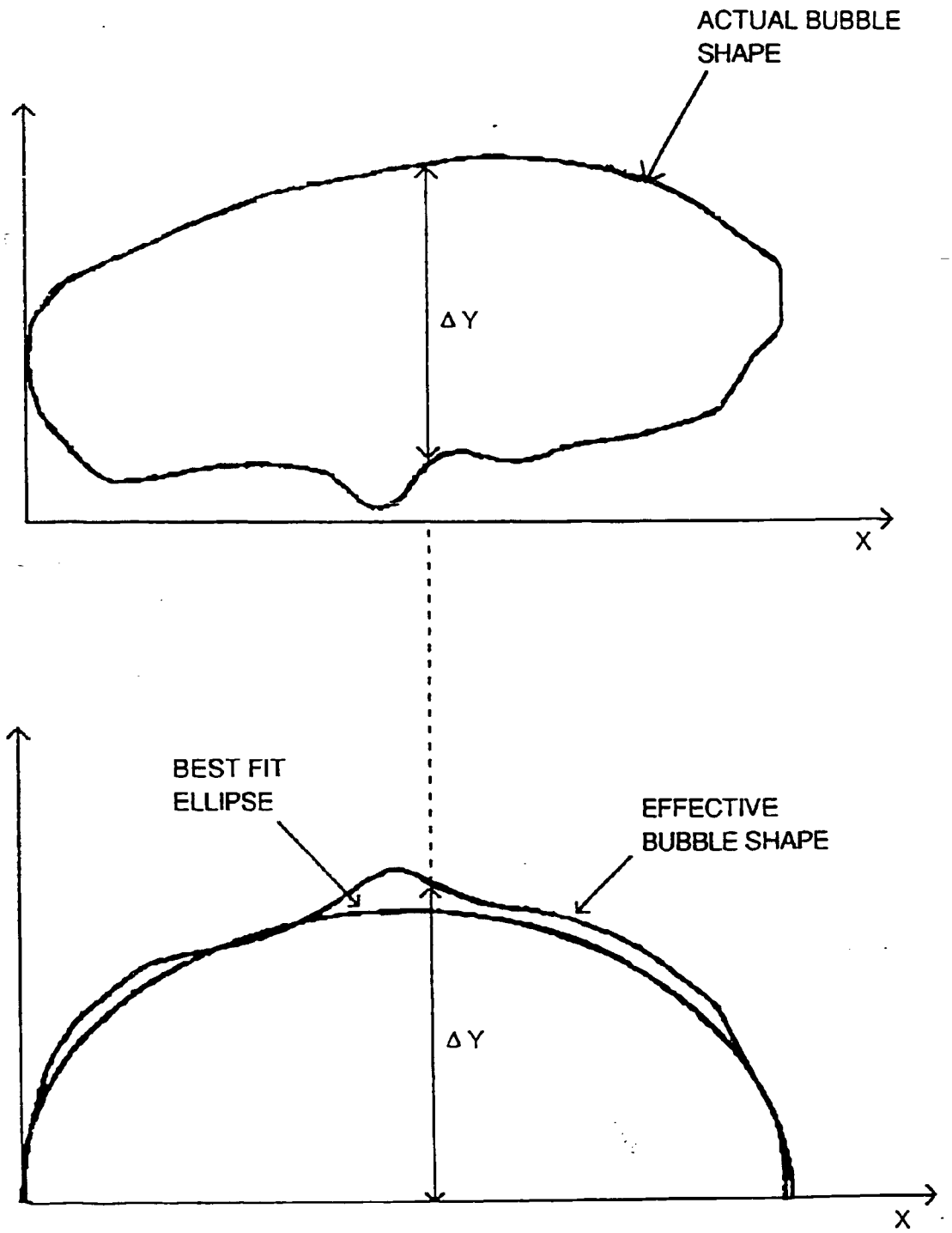

Figure 3: Approximating the effective bubble shape with a best fit ellipse. This technique was used to generate the data shown in figures 4 and 6.

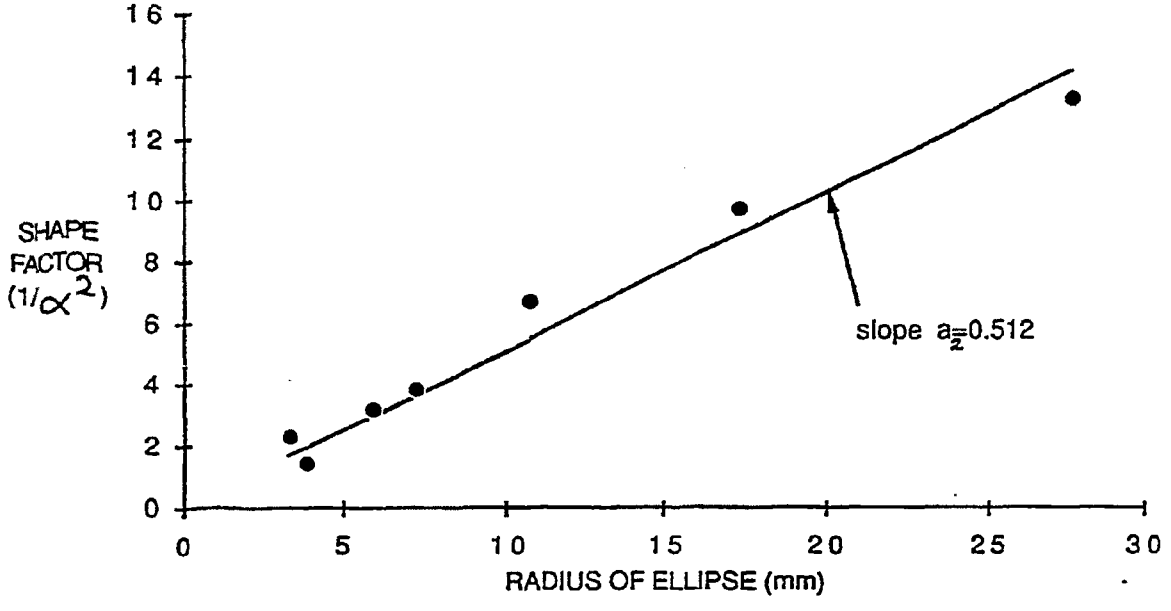

Figure 4: Variation of bubble shape with respect to size. The points refer to our measurements of photographs of bubbles presented in Batchelor's book.

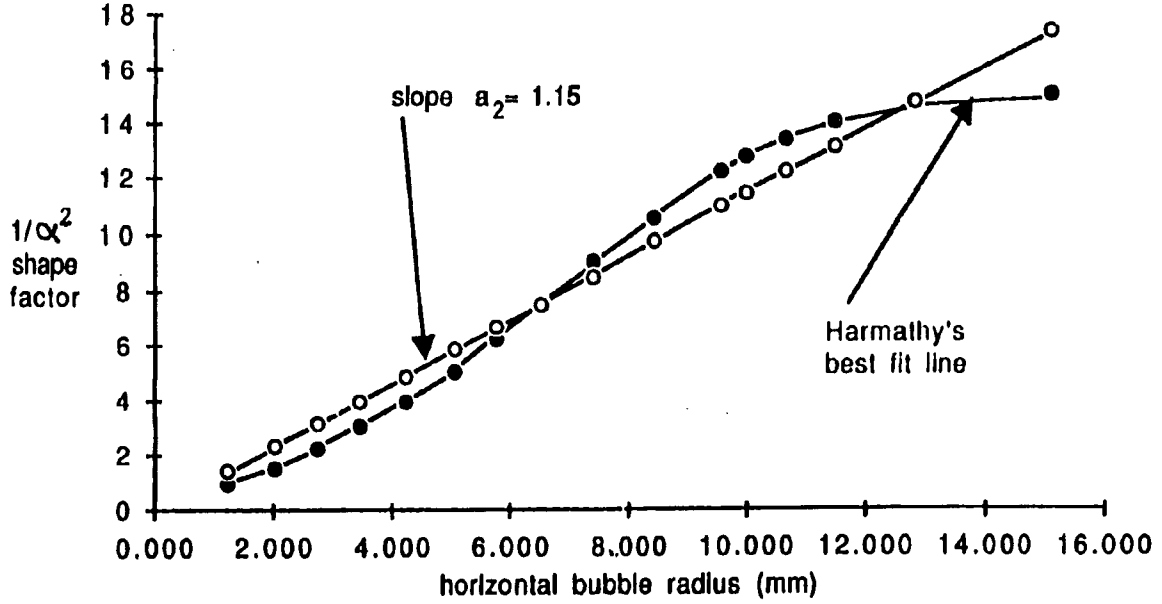

Figure 5: Variation of bubble shape with size for air-water systems, based on a "best fit" line proposed by Harmathy. This has in turn been approximated with the linear relationship of equation 2.

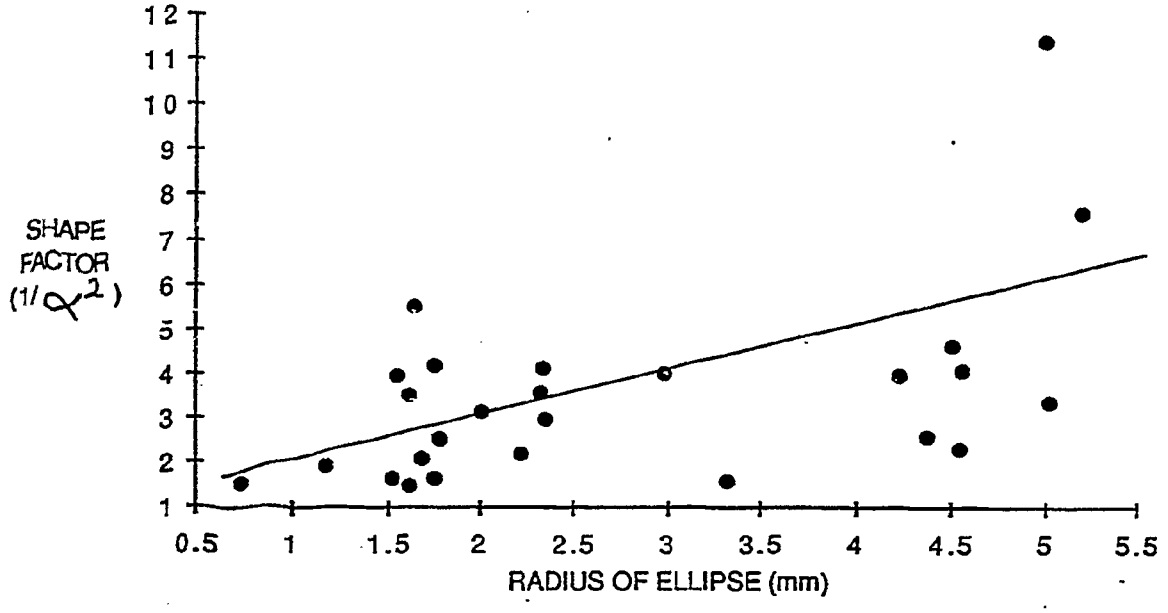

Figure 6: Variation of bubble shape with size. The points refer to our data taken from bubbles in a glass column. The line represents the best fit to Harmathy's data, as shown in figure 5.

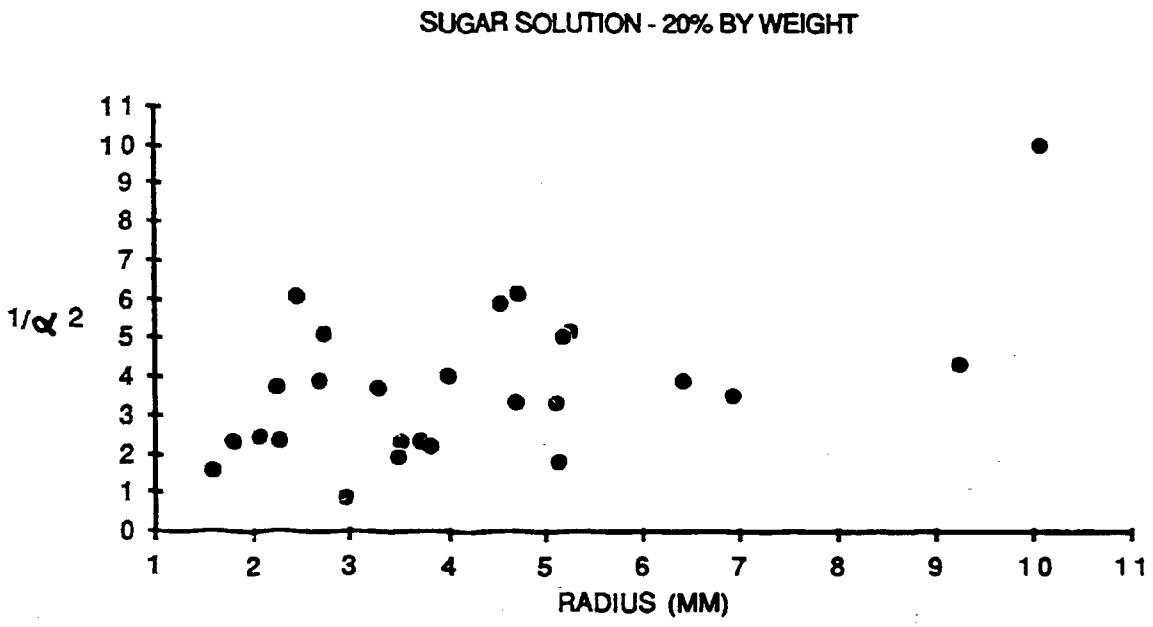

Figure 7: Variation of bubble aspect ratio as a function of bubble size for a 20% sugar solution. Bubbles are generally flatter than with air-water systems.

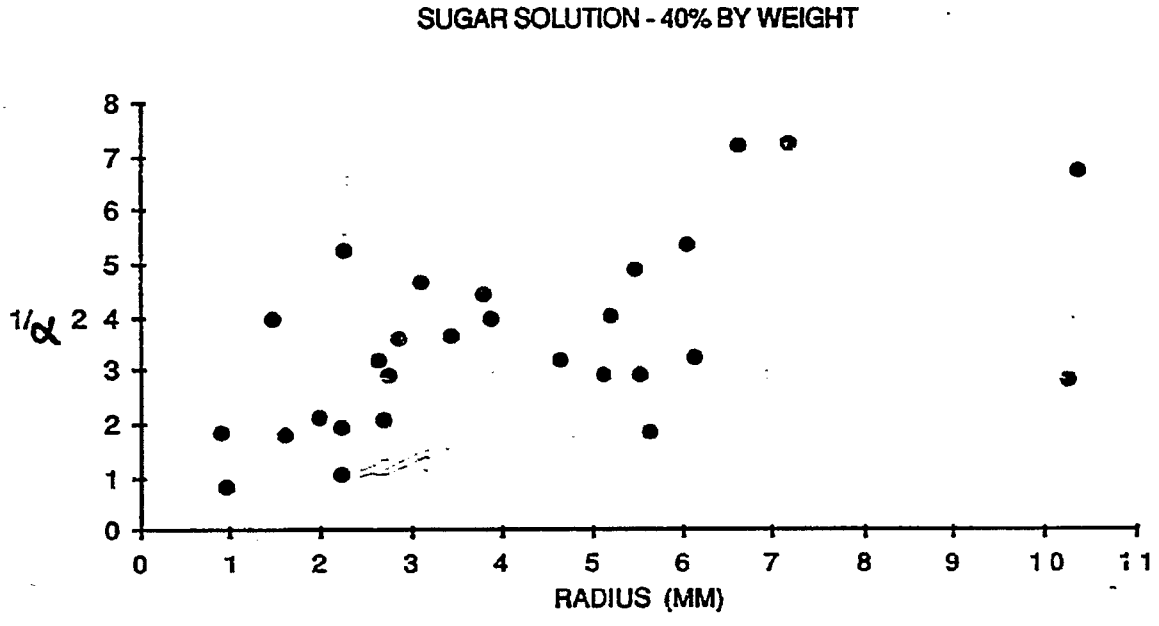

Figure 8: Bubble shapes in a 40% sugar solution.

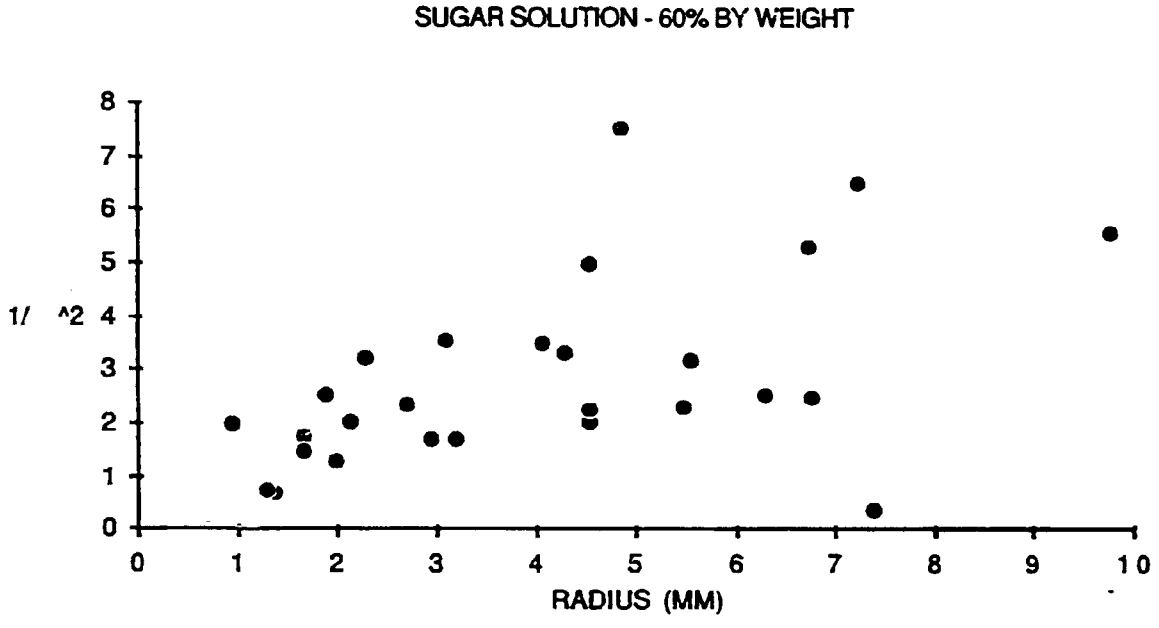

Figure 9: Bubble shapes in a 60% sugar solution.

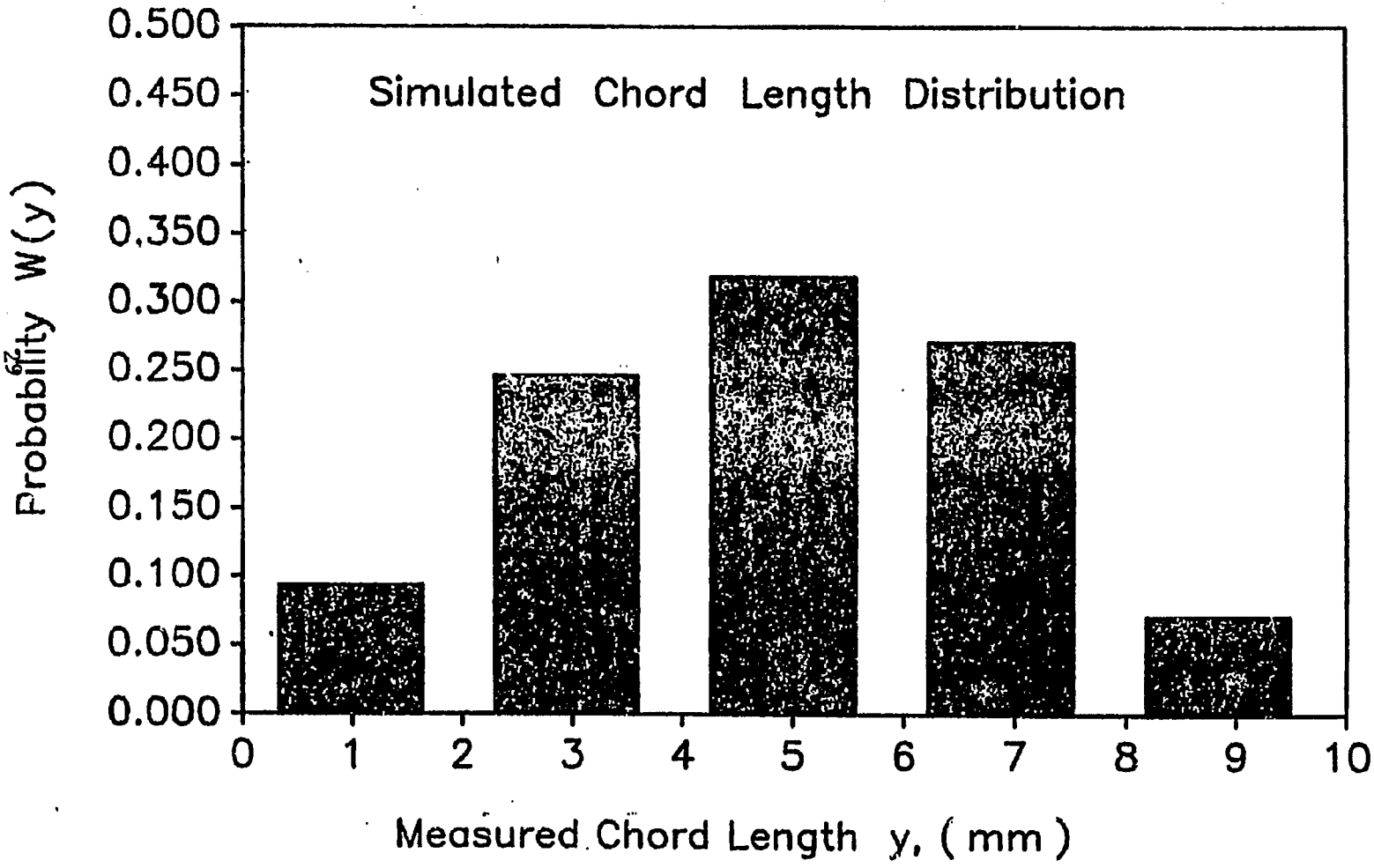

Figure 10.
The Chord length distribution generated for a simulation using 3000 bubbles from a triangular distribution with R_{max} = 30mm and a mode of 18mm (5 divisions).

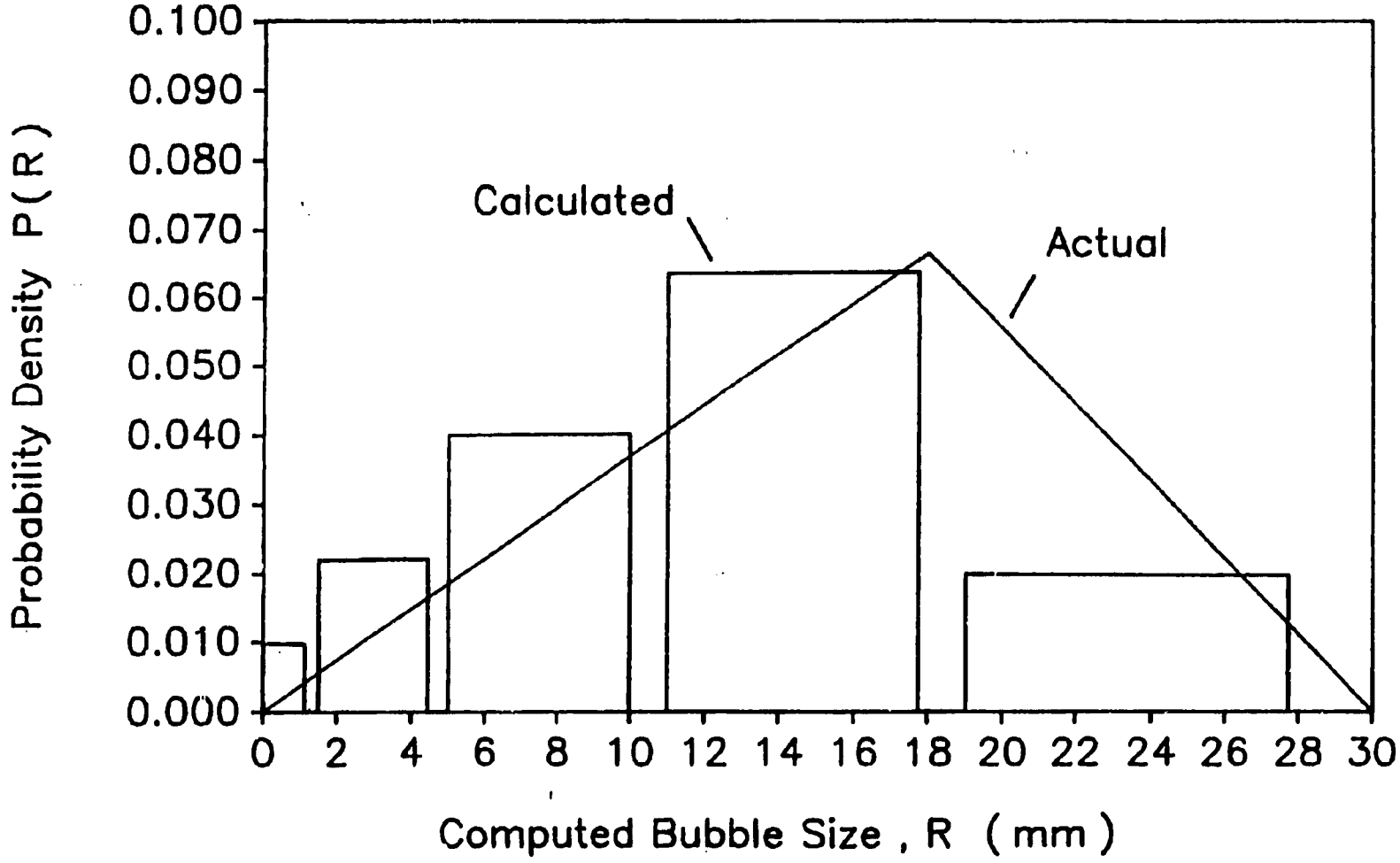

Figure 11.
The bubble size distribution obtained by back transforming the chord length distribution shown in Figure 6.

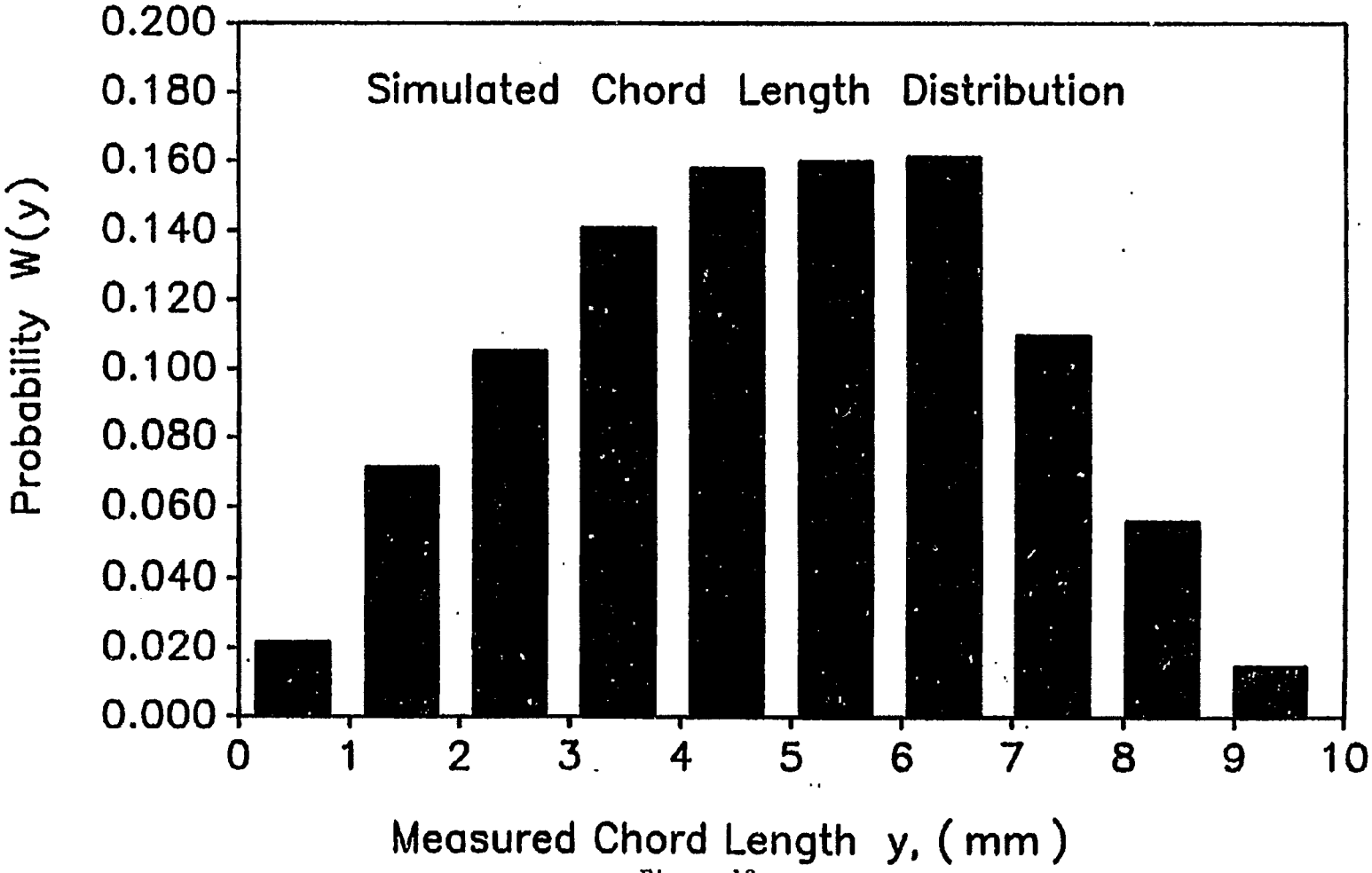

Figure 12.
The chord length distribution generated for a simulation using 3000 bubbles from a triangulr distribution with R_{max} = 30mm and mode of 18mm (10 divisions)

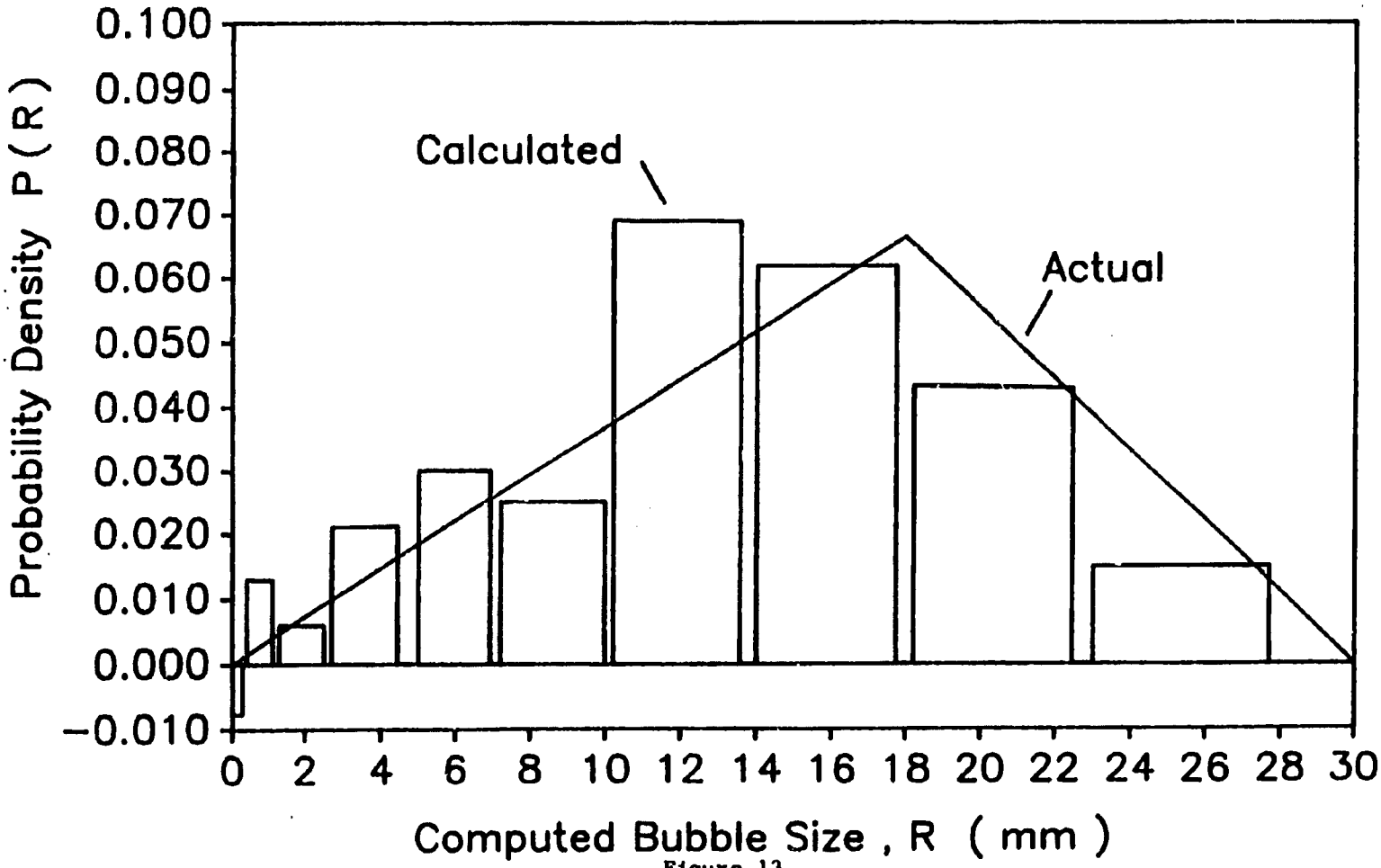

Figure 13.

The bubble size distribution obtained by back transforming the chord length distribution shown in Figure 8.

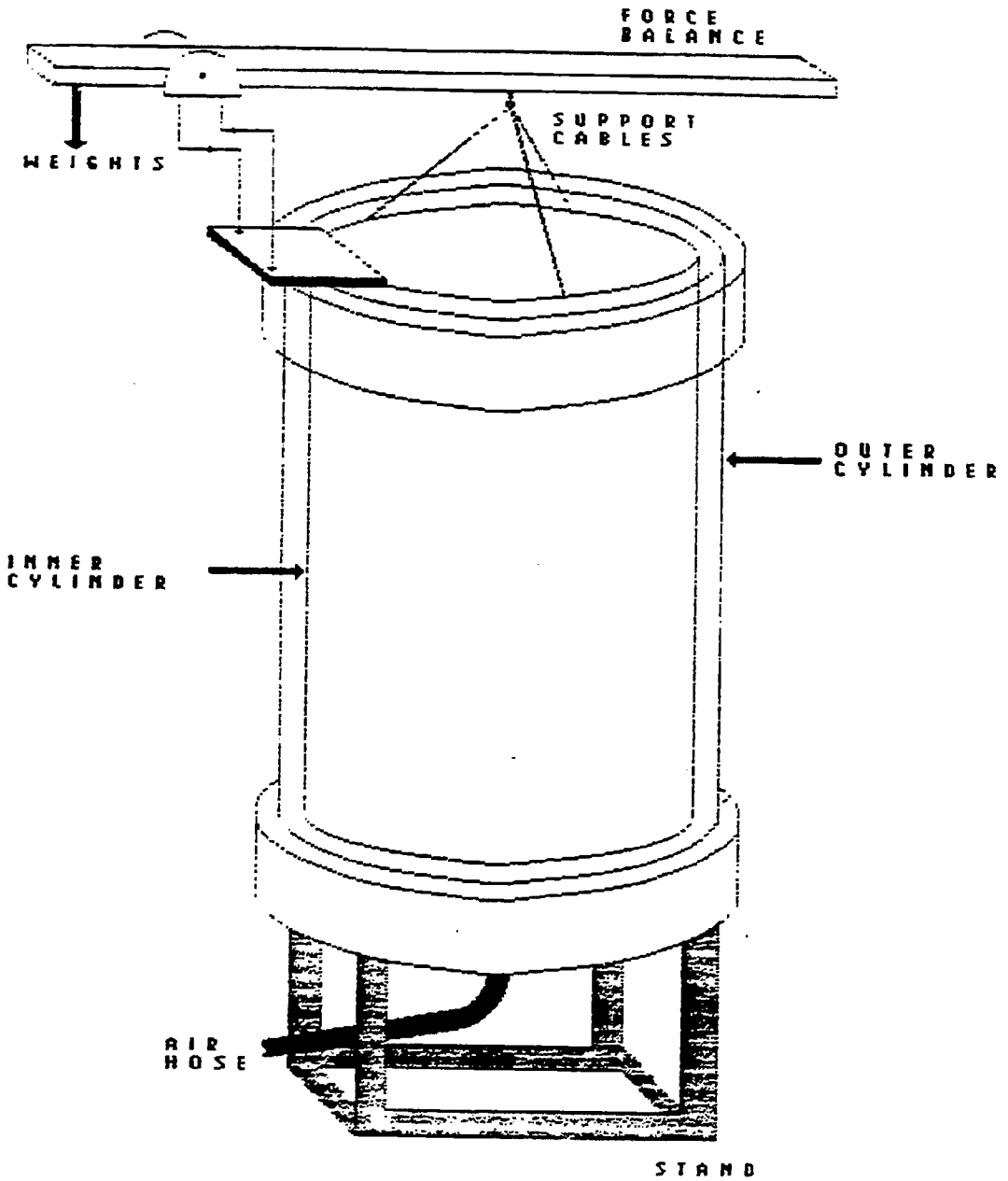

Figure 14: Measurement of wall shear with a suspended cylinder and balance arm: schematic of apparatus currently in use.

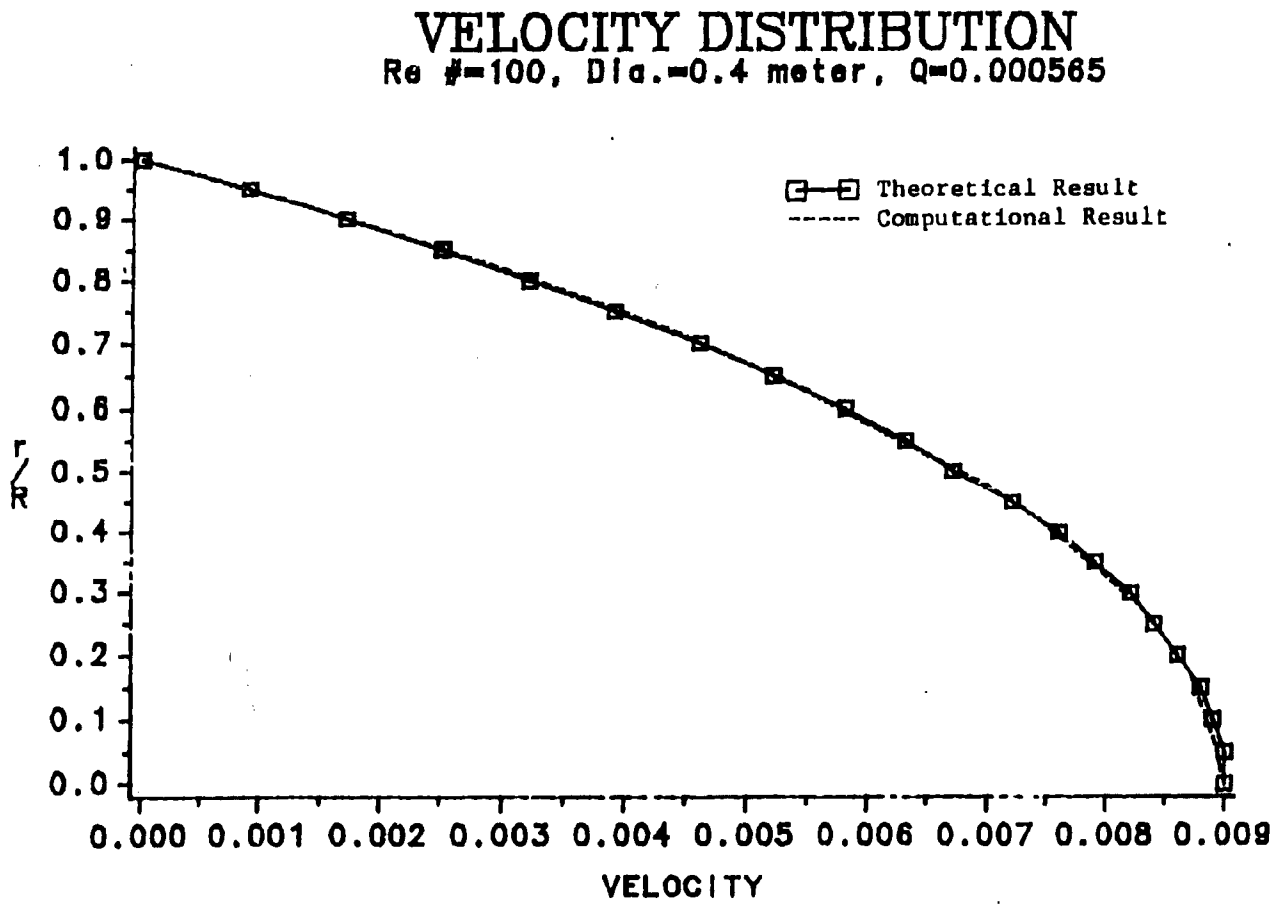

Fig. 15 Computed and Theoretical Velocity Distributions for a Single Phase Flow in a 0.4-m-Diameter Vertical Pipe.

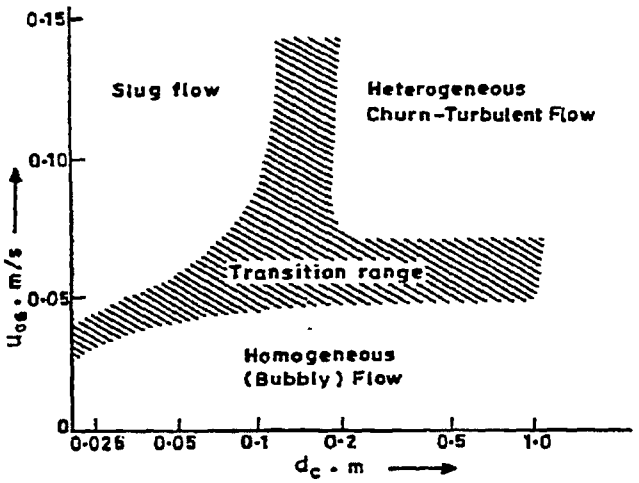

Fig. 16.a Approximate Dependency of Flow Regime on Gas Velocity and Column Diameter (Water and Dilute Aqueous Solution). (After Shah et al, 1982)

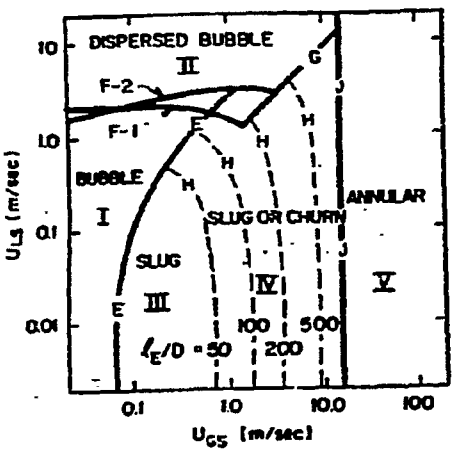

Fig. 16.b Flow-Pattern Map: Upward Air-Water Flow (at 1 atm.) in a 5.1-cm-Diameter Tube. (After Dukler et al, 1986)

U.S. DEPARTMENT OF COMMERCE
Technology Administration
National Technical Information Service
Springfield, VA 22161 (703) 605-6000